Technical Note

The Impact of the Grid Size on TomoTherapy for Prostate Cancer

Motohiro Kawashima, Hidemasa Kawamura[1], Masahiro Onishi[1], Yosuke Takakusagi[2], Noriyuki Okonogi[1,3], Atsushi Okazaki[2], Tetsuo Sekihara[2], Yoshitaka Ando[2], Takashi Nakano[1]

Gunma University Heavy Ion Medical Center, Maebashi, [1]Department of Radiation Oncology, Gunma University Graduate School of Medicine, Maebashi, [2]Hidaka Hospital, Takasaki, Gunma, [3]Hospital, National Institute of Radiological Sciences, National Institutes for Quantum and Radiological Science and Technology, Japan

Abstract

Discretization errors due to the digitization of computed tomography images and the calculation grid are a significant issue in radiation therapy. Such errors have been quantitatively reported for a fixed multifield intensity-modulated radiation therapy using traditional linear accelerators. The aim of this study is to quantify the influence of the calculation grid size on the dose distribution in TomoTherapy. This study used ten treatment plans for prostate cancer. The final dose calculation was performed with "fine" (2.73 mm) and "normal" (5.46 mm) grid sizes. The dose distributions were compared from different points of view: the dose-volume histogram (DVH) parameters for planning target volume (PTV) and organ at risk (OAR), the various indices, and dose differences. The DVH parameters were used Dmax, D2%, D2cc, Dmean, D95%, D98%, and Dmin for PTV and Dmax, D2%, and D2cc for OARs. The various indices used were homogeneity index and equivalent uniform dose for plan evaluation. Almost all of DVH parameters for the "fine" calculations tended to be higher than those for the "normal" calculations. The largest difference of DVH parameters for PTV was Dmax and that for OARs was rectal D2cc. The mean difference of Dmax was 3.5%, and the rectal D2cc was increased up to 6% at the maximum and 2.9% on average. The mean difference of D95% for PTV was the smallest among the differences of the other DVH parameters. For each index, whether there was a significant difference between the two grid sizes was determined through a paired *t*-test. There were significant differences for most of the indices. The dose difference between the "fine" and "normal" calculations was evaluated. Some points around high-dose regions had differences exceeding 5% of the prescription dose. The influence of the calculation grid size in TomoTherapy is smaller than traditional linear accelerators. However, there was a significant difference. We recommend calculating the final dose using the "fine" grid size.

Keywords: Calculation grid size, dose distribution, TomoTherapy, treatment planning

Received on: 24-11-2016 **Review completed on: 19-06-2017** **Accepted on: 11-07-2017**

Introduction

Intensity-modulated radiation therapy (IMRT)[1] and volumetric-modulated arc therapy[2,3] are performed in many radiation treatment facilities. A specialized IMRT device called "helical TomoTherapy"[4-6] has been developed in the early 1990s. The TomoTherapy Hi-Art system (Accuray Inc., Sunnyvale, CA, USA) combines delivery of intensity-modulated fan-beam rotational therapy with megavoltage computed tomography (CT) imaging capabilities. The nominal energy of the photon beam is 6 MV, there is no flattening filter, and the beam is cone shaped. The irradiation beam has a maximum lateral width of 40 cm at the isocenter plane, and this beam is shaped by an adjustable jaw and a binary multileaf collimator (MLC). The longitudinal field size after adjusting the jaw can be set to 1.0, 2.5, or 5.0 cm. The MLC consists of 64 binary leaves. A length of one binary leaf is 0.625 cm at the isocenter plane. The TomoTherapy treatment planning system (TPS), "TomoTherapy Planning Station," determines the treatment plan parameters (e.g., the field width, pitch factor, and modulation factor) and optimizes the beam for irradiating the target while sparing normal tissue. A final dose calculation is performed after optimization. TomoTherapy uses a convolution/superposition algorithm to compute dose and utilizes a proprietary inverse planning optimization

Access this article online

Quick Response Code:

Website: www.jmp.org.in

DOI: 10.4103/jmp.JMP_123_16

Address for correspondence: Dr. Motohiro Kawashima, Gunma University Heavy Ion Medical Center, Maebashi, Gunma, Japan.
E-mail: mkawashi@gunma-u.ac.jp

How to cite this article: Kawashima M, Kawamura H, Onishi M, Takakusagi Y, Okonogi N, Okazaki A, *et al*. The impact of the grid size on tomotherapy for prostate cancer. J Med Phys 2017;42:144-50.

algorithm.[7,8] During the optimization and dose calculation, the grid size can be set to "fine," "normal," or "coarse." The resolution of the fine grid size is down sampled (256 × 256) from CT images (512 × 512) in the axial plane. The resolutions of normal and coarse grid sizes are downsampled to half (128 × 128) and quarter (64 × 64) that of the fine resolution, respectively. The longitudinal resolution of all the grid sizes is the same as the slice thickness.

Macroscopically, the dose distribution is continuous in nature. However, the dose distribution calculated in the TPS is discretized. Therefore, the calculated dose distribution has inherent errors associated with discretization. The calculation grid size is one of the major determinants of the accuracy of the TPS.[9-11] The effects of these errors have been quantitatively evaluated for a fixed multifield IMRT using traditional linear accelerators. TomoTherapy has a different irradiation method from fixed multifield IMRT. Therefore, the impact of the grid size on TomoTherapy may be different. In this study, a quantitative evaluation of the dose distribution influenced by the grid size was performed.

Materials and Methods

Five patients each Stage II and Stage III prostate cancer cases were used for this study. Radiation oncologists created contours of planning target volume (PTV) and organ at risk (OAR; i.e., rectum and bladder) for all CT images.[12] Okonogi *et al*. described how to contour delineation in the paper. One oncologist specializing in prostate cancer checked these contours. The CT images (3-mm slices) were acquired using an Aquilion LB 16 (Toshiba Medical Systems, Otawara, Tochigi, Japan). Scanning was performed at the X-tube voltage of 120 kV, tube current of 150 mA, and helical pitch of 15 mm/rot. Treatment plans were designed using these images and contours in TomoTherapy Planning Station version 4.2.3 (Tomotherapy Incorporated, Madison, WI, USA) and were transferred to the treatment device in the network.

The prescription dose for the treatment plan was 78 Gy at 2 Gy/fraction. The treatment plan was optimized using dose constraints of the PTV and OAR. The dose constraints of the PTV stipulated that the dose prescription method was D95% (prescription dose covered 95% volume of PTV) and that the D2cc (the minimum dose to the highest irradiated 2-cc volume) was no >105% of the prescription dose (D2cc <81.9 Gy). The dose constraints of OAR stipulated that D17% <65 Gy, D35% <40 Gy, and D60% <22 Gy (Dx% indicates the dose covering x% of the total volume) for the rectum and D25% <65 Gy and D50% <40 Gy for the bladder. The parameters in all treatment plans were set to same value. The field width, pitch, and modulation factor were set to 0.25, 0.287, and 2.0 in all treatment plans, respectively. The field width represents the longitudinal width of the jaw with a unit of mm/100. The pitch factor is the axial couch travel distance for one gantry rotation divided by the field width. The modulation factor is defined as the ratio of the maximum leaf open time to the average leaf open time. Here, this factor was set to ensure that maximum leaf open time was not more than twice the average leaf open time.

The grid size may be selected from among fine, normal, and coarse settings in the optimization and dose calculation. These grid sizes have an inverse relationship to the pixel size of the CT image, which is affected by the field of view (FOV). In this study, CT images were taken with a 700-mm FOV. Therefore, the fine, normal, and coarse grid sizes were 2.73, 5.46, and 10.92 mm in the axial plane, respectively. Dosimetric validation tests described in task group 148, of the American Association of Physicists in Medicine, indicated that the normal grid should be used as the reference grid size.[13] Therefore, because the course is less accurate than the normal, it was excluded from the comparison performed in this study.

The optimization of treatment plans was performed using the normal grid size in all treatment plans. Thereby, an MLC movement sequence was same for each patient. The final dose distributions were calculated using the normal and fine grid sizes after optimization.

The comparison of treatment plans calculated using the fine and normal grid sizes was performed using dose-volume histogram (DVH) dose parameters. Dmax, D2%, D2cc, Dmean, D95%, D98%, and Dmin were used to evaluate the dose coverage of PTV. Dmax, D2%, and D2cc for OARs (rectum and bladder) were used to evaluate dose differences. We also used the homogeneity index (HI)[14] and equivalent uniform dose (EUD)[15] as to evaluate the plan.

The HI is represented by the following equation:

$$HI = \frac{D_{2\%} - D_{98\%}}{Prescribed\ \ Dose} \times 100 \quad (1)$$

where D2% and D98% are doses to 2% and 98% volumes of the PTV, respectively. HI becomes zero under ideal conditions. This index represents the uniformity of the dose in the PTV. We used the reference dose evaluation for high-precision treatment, as defined in the International Commission on Radiation Units and Measurements Report 83.[14]

The EUD is defined by the following formula:

$$EUD = 2Gy\ \ln\left[\frac{1}{N}\sum_{i=1}^{N}\left(SF_2\right)^{D_i/2Gy}\right]\Big/\ln\left(SF_2\right) \quad (2)$$

Where SF_2 is the survival fraction at 2 Gy. We assumed the SF_2 to be 0.5 in this study. N indicates the number of computational grid cells, and i is the index of the grid cell.

These indices were used to evaluate the treatment plan. We also performed a two-tailed paired *t*-test to verify whether there was a significant difference between the calculations based on the fine and normal grids. The confidence interval was set to 95%.

We calculated the difference between the dose distributions calculated using fine and normal grid sizes at the isocenter plane. The difference between the dose distributions was

obtained by subtracting the dose distribution calculated using the normal grid size from that calculated using the fine grid size. These calculations were performed using the MIM Maestro software package (MIM Software Inc., Cleveland, OH, USA). The result was illustrated by plotting a histogram of dose difference.

In addition, the calculated dose distributions were compared with EBT3 Gafchromic film measurement to evaluate the accuracy of the treatment plans.[16,17] The Gafchromic film dosimetry validated the prescribed dose delivery to within ±5% (one standard deviation). The gamma evaluation method was used to compare dose distributions with 3% dose difference and 3-mm distance-to-agreement criteria.[18] The threshold was set to 30% in this study because the EBT3 has the larger uncertainty in the low-dose region. We compared the relative dose distributions normalized at the isocenter. These analyses were performed with the MapCHECK software package called SNC Patient version 6.1.1 (Sun Nuclear Corp., Melbourne, FL, USA). In addition, we verified whether similar DVH parameters for PTV could be obtained in three head and neck (HN) cases.

Results

The calculated treatment plans were compared using the DVH [Figure 1]. The DVH calculated using the fine and normal grid sizes are represented by dotted and solid lines, respectively. In addition, we showed an expanded view of the high-dose region. The maxima of the DVHs were larger in the plan calculated using the fine grid than in the plan calculated using the normal grid.

The DVH parameters for the PTV and OAR are summarized in Tables 1 and 2, respectively, for all cases. The average differences of Dmax, D2%, D2cc, Dmean, D95%, D98%, and Dmin for PTV were 3.5%, 1.9%, 1.6%, 0.6%, 0.4%, 0.9%, and 1.4% of prescription dose, respectively. The maximum differences of Dmax, D2%, D2cc, Dmean, D95%, D98%, and Dmin for PTV were 5.3%, 2.4%, 1.9%, 0.8%, 0.6%, 4.5%, and 4.2%. Overall, DVH parameters calculated with the fine grid size were greater than those calculated with the normal grid and were significantly different according to a two-tailed paired *t*-test. The differences in D98% and Dmin were not statistically significant. The DVH parameters of the rectum and bladder had results similar to those of the PTV. The average of rectal D2cc was increased by 2.9%, and maximum differences were 6.0% for patient 3. All DVH parameters for OAR indicated statistically significant differences according to a two-tailed paired *t*-test.

We present the indices for plan evaluation, HI and EUD, in Table 3. The D2% and D98% that was used to calculate HI increased when using the fine grid size. The mean HI obtained with the fine grid was 1.01 times greater than that obtained with the normal grid. The EUD calculated using the fine grid increased by approximately 0.5% of the prescription dose relative to that calculated using the normal grid size and exhibited a significant difference according to a two-tailed paired *t*-test.

The DVH has no information about location of the CT image. Therefore, we did not know where the dose difference indicated

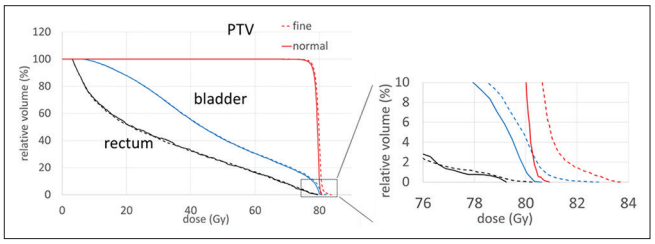

Figure 1: Cumulative dose-volume histograms of treatment plans calculated using the fine and normal grid sizes, illustrating the dose to the planning target volume, rectum and bladder and an expanded view of the high-dose region. The two types of dose-volume histogram are generally similar in form

Table 1: Dose-volume histogram parameters for planning target volume

Patient number	Dmax		D2%		D2cc		Dmean		D95%		D98%		Dmin	
	Normal	Fine	Normal	Fine	Normal	Fine	Normal	Fine	Normal	Fine	Normal	Fine	Normal	Fine
1	103.0	106.9	102.5	104.5	102.4	104.3	101.2	101.9	100.0	100.5	99.2	99.9	94.9	96.3
2	103.5	105.2	102.5	104.0	102.4	103.8	101.1	101.8	99.8	100.3	94.9	99.4	86.6	82.4
3	102.8	106.2	102.3	104.3	102.1	103.8	101.0	101.7	100.0	100.0	99.5	99.6	95.6	98.4
4	103.7	106.5	103.2	104.9	103.1	104.5	101.9	102.5	100.2	100.7	99.0	99.6	93.2	96.0
5	103.0	106.9	102.7	104.1	102.6	103.9	101.6	102.1	99.9	100.1	99.0	99.2	92.6	96.0
6	103.4	106.0	102.9	104.5	102.8	104.2	101.6	102.3	100.0	100.6	99.2	99.7	94.2	97.4
7	103.7	107.3	103.0	104.7	103.0	104.9	101.5	102.1	99.5	99.9	98.3	99.0	87.8	91.9
8	103.2	107.1	102.7	104.8	102.5	104.2	101.4	102.1	100.0	100.3	98.8	99.7	94.2	93.6
9	103.4	106.7	103.0	105.4	102.9	104.7	101.6	102.3	100.0	100.0	99.4	99.4	96.0	97.0
10	103.8	109.1	103.2	105.6	103.1	104.9	101.8	102.6	100.0	100.4	98.3	99.1	93.0	93.1
Mean±SD	103.3±0.3	106.8±1.0	102.8±0.3	104.7±0.5	102.7±0.4	104.3±0.4	101.5±0.3	102.1±0.3	99.9±0.2	100.3±0.3	98.6±1.3	99.5±0.3	92.8±3.2	94.2±4.6
P	<0.001		<0.001		<0.001		<0.001		<0.001		0.059		0.114	

This table lists the DVH parameters, average and SD of all cases. The *P* values between the fine and normal groups are shown. The unit of all data excluding the *P* values is percentage. DVH: Dose-volume histogram, PTV: Planning target volume, Dmax: Maximum dose, Dmean: Mean PTV dose, Dmin: Minimum dose irradiated to the PTV, SD: Standard deviation, Dx%/cc: The minimum dose to the highest irradiated x-%/cc volume

Table 2: Dose-volume histogram parameters for the rectum and bladder

Patient number	Rectum						Bladder					
	Dmax		D2%		D2cc		Dmax		D2%		D2cc	
	Normal	Fine	Normal	Fine	Normal	Fine	Normal	Fine	Normal	Fine	Normal	Fine
1	102.1	106.0	100.5	101.3	99.1	101.3	102.6	103.8	101.1	101.7	102.0	102.7
2	101.7	103.4	100.1	101.0	99.9	101.0	102.3	104.6	101.3	101.9	102.0	102.7
3	101.7	104.5	101.6	102.0	96.0	102.0	101.7	104.4	101.5	102.3	101.5	102.3
4	102.8	104.2	101.8	102.2	101.2	102.2	102.9	104.7	102.7	103.2	102.7	103.3
5	102.6	106.5	101.0	101.7	99.0	101.7	102.6	103.5	101.5	101.9	102.3	103.0
6	102.2	104.4	101.2	101.8	99.3	101.8	102.8	105.3	101.8	102.4	102.5	103.1
7	101.2	102.5	98.1	97.9	95.2	97.9	103.0	105.9	102.4	103.1	102.7	103.6
8	102.3	106.1	100.9	102.6	98.3	102.6	102.2	105.7	101.8	102.5	102.1	102.8
9	102.4	105.2	99.7	99.7	96.2	99.7	103.0	105.2	102.5	104.0	101.7	102.6
10	102.7	105.7	101.3	102.2	98.2	102.2	103.2	105.7	102.5	103.2	102.8	103.6
Mean±SD	102.2±0.5	104.9±1.3	100.6±1.1	101.2±1.4	98.3±1.9	101.2±1.4	102.6±0.5	104.9±0.8	101.9±0.6	102.6±0.7	102.2±0.5	103.0±0.4
P	<0.001		0.003		<0.001		<0.001		<0.001		<0.001	

This table lists the DVH parameters, averages and SDs of all cases. The *P* values between the fine and normal groups are shown. The unit of all data excluding the *P* values is percentage. DVH: Dose-volume histogram, Dmax: Maximum dose, SDs: Standard deviations, Dx%/cc: The minimum dose to the highest irradiated x-%/cc

Table 3: Homogeneity index and equivalent uniform dose values for all cases

Patient number	HI		EUD	
	Normal	Fine	Normal	Fine
1	3.29	4.59	2.02	2.04
2	7.54	4.59	2.02	2.04
3	2.78	4.7	2.02	2.03
4	4.28	5.36	2.04	2.05
5	3.63	4.94	2.03	2.04
6	3.68	4.82	2.03	2.05
7	4.71	5.7	2.03	2.04
8	3.91	5.11	2.03	2.04
9	3.54	5.96	2.03	2.05
10	4.89	6.54	2.04	2.05
Mean±SD	4.22±1.33	5.23±0.66	2.03±0.01	2.04±0.01
P	0.057		<0.001	

HI: Homogeneity index, EUD: Equivalent uniform dose, SD: Standard deviation

by DVH difference was on the CT images. The dose difference distribution was obtained by subtracting calculation with normal grid from that with the fine grid size. Figure 2 shows the dose distribution of one patient calculated using the fine grid size. Figure 3 shows the difference between the dose distributions calculated using the fine and normal grid sizes. The large difference evident in Figure 3 was located at the steep-dose gradients shown in Figure 2. There is difference of more than 5% between calculated dose using fine and normal grid.

The histogram represents the dose difference between distributions calculated with fine and normal grid sizes [Figure 4]. We found that the dose distributions were consistent overall. The mean dose difference was 0.03% of the prescribed dose, and the variation was 0.56%. The results for the fine grid size dose were slightly higher than for the normal.

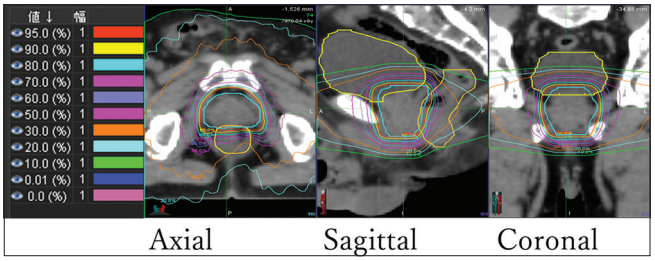

Figure 2: Dose distribution calculated using the fine grid size. The isodose lines contours are defined according to the relative prescription dose

The calculation accuracy was evaluated by performing film measurements. We compared calculations with measurements through gamma analysis that acceptance criteria were 3%/3 mm. The pass rates, which were derived from comparisons of calculations and film measurement, were approximately the same. We generated a histogram of the percentage dose difference between each calculation and the EBT3 measurement, as shown in Figure 5a and b. The Figure 5a and b show the dose differences between the calculations with normal and fine grid sizes, respectively, and the measurements. The Figure 5a has a wider distribution than the Figure 5b. The calculations that used the fine grid size were found to be more consistent than for those that used the normal grid size.

The comparison of DVH parameters between prostate and HN cases is summarized in Table 4. The treatment plans for HN require stronger modulation than those for the prostate due to the proximity of critical structures, the spinal cord, and parotid glands. However, the variation of DVH parameters excluding Dmax for PTV in HN case was not so different from one in prostate. In contrast, the difference between the Dmax calculated with normal and fine grid for HN cases was much larger than that for prostate cases.

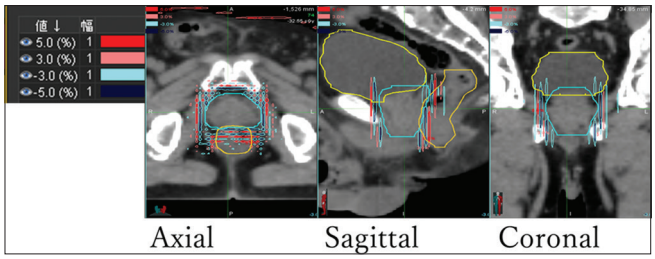

Figure 3: Difference between the dose distributions calculated using the fine and normal grid sizes. These differences were obtained by subtracting the dose distribution calculated using the normal grid size from that calculated using the fine grid size. The isodose contours are defined according to the relative prescription dose

Table 4: Comparison of dose-volume histogram parameters between prostate and head and neck cases

	Prostate	HN
Dmax		
Normal	103.3	105.6
Fine	106.8	111.0
Differential	3.5	5.5
D2%		
Normal	102.8	103.7
Fine	104.7	104.7
Differential	1.9	1.0
D2cc		
Normal	102.7	103.9
Fine	104.3	105.2
Differential	1.6	1.3
Dmean		
Normal	101.5	101.6
Fine	102.1	102.0
Differential	0.6	0.3
D95%		
Normal	99.9	99.2
Fine	100.3	99.4
Differential	0.4	0.2
D98%		
Normal	98.6	97.5
Fine	99.5	98.0
Differential	0.9	0.5
Dmin		
Normal	92.8	83.6
Fine	94.2	82.2
Differential	1.4	−1.4

The unit is relative prescription dose. Dmax: Maximum dose, HN: Head and neck, Dmean: Mean PTV dose, Dmin: Minimum dose irradiated to the PTV, PTV: Planning target volume, Dx%/cc: The minimum dose to the highest irradiated x-%/cc volume

Discussion

We assessed the treatment plans from several perspectives to quantify the influence of the calculation grid size on the dose distribution in TomoTherapy. The differences in the various DVH parameters and dose indices of the calculation using fine and normal grid sizes were statistically significant. Moreover,

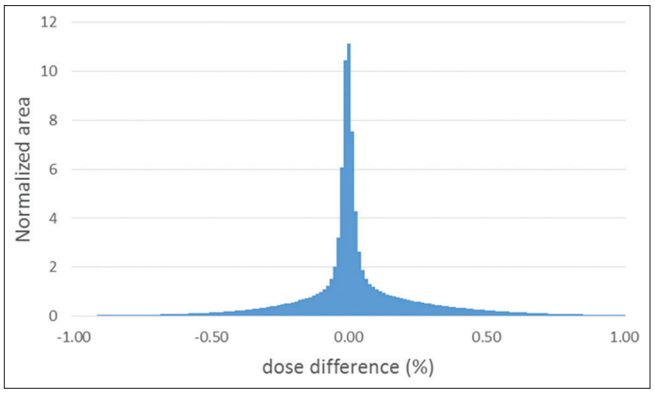

Figure 4: Frequency histogram of the difference between the doses calculated using the fine and normal distributions. The height corresponds to the ratio of the number of voxels. The horizontal axis represents the relative prescription dose. The bin width is 0.01%

we compared film's measurements with calculated dose distribution using each grid size. Since fine grid size is more consistent with real film measurements, it is better to generate radiation treatment plan using fine grid size instead of normal grid size. On the other hand, the dose distribution obtained using the normal grid size is very useful in the clinic because it can be generated in a short time. The time required to calculate the final dose with the fine grid size is approximately four times that for the normal grid size. For example, the average computational times for the normal and fine grid sizes were 1.5 and 5.6 min, respectively, in this work. However, if the normal organ dose is barely tolerable in the treatment plan with the normal grid size, there is a high probability that the actual irradiation dose exceeds the tolerance dose. This is particularly important for serious toxicity of serial organs. On this basis, if time permits, we recommend performing calculations using the fine grid size for improved accuracy.

A previous study for traditional linear accelerator has reported similar conclusions.[11] Chung *et al.* found that the overall dose distribution was shifted to higher values when the grid size is increased, and the D95% obtained using a 4-mm grid size was 2.6% greater than that obtained using a 2-mm grid size. Although the fine and normal grid sizes are 2.73 mm and 5.46 mm, respectively, there is a 0.4% and 0.2% prescription difference between the D95% values obtained using the different grid sizes for prostate and HN cases, respectively. We considered that this difference emerges from irradiation method. The influence of the DVH parameters in TomoTherapy is smaller those that in fixed-field IMRT.

TomoTherapy Planning Station calculates the dose distributions using the average CT values of pixels in the grid.[19] The current study verified the dose calculation at the pelvic region. There were no large differences among the CT values in this region. However, treatment plans for the lung region, for which there are large differences among the CT values, may exhibit a greater dose calculation error. Because there is a possibility that the influence of the grid size may differ in lung cases, future studies may be needed to verify these results.

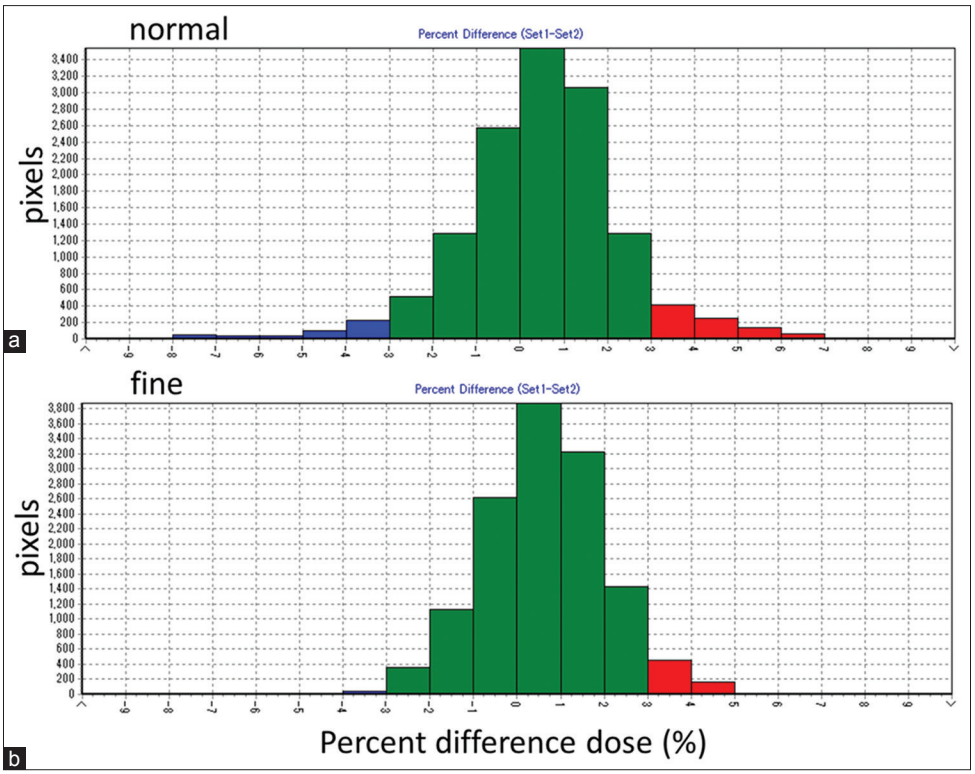

Figure 5: Histogram of the difference between the dose measurement and calculation. The height corresponds to the grid number. The bin width is 1%. The (a and b) figures represent the difference between the measurement and the calculations calculation with the normal and fine grid sizes, respectively

Conclusions

The calculation grid size is one of the major determinants of the accuracy of the TPS. The selection of grid size is very important for reducing generation times of treatment plans, too.

The overall dose distribution was almost identical regardless of the grid size, and the variations of DVH parameters for TomoTherapy were smaller than those fixed for multifield IMRT. However, the D2% of the PTV and D2cc of the OAR, which are often used for treatment plan evaluation, were significantly changed by the grid size. TomoTherapy, a specialized IMRT device, is a high-precision treatment machine.

Therefore, we recommend that the "fine" calculation grid size be used for dose computation, at least.

Acknowledgments

We thank Mikio Irie, Shinichi Ueki, and Takuya Suda for helping with film measurements and chamber to verify the treatment plans. We also acknowledge support regarding the TomoTherapy software operations from the Department of Applications in Hitachi Medico Corporation.

Financial support and sponsorship

Nil.

Conflicts of interest

There are no conflicts of interest.

References

1. Webb S. The physical basis of IMRT and inverse planning. Br J Radiol 2003;76:678-89.
2. Otto K. Volumetric modulated arc therapy: IMRT in a single gantry arc. Med Phys 2008;35:310-7.
3. Bortfeld T, Webb S. Single-Arc IMRT? Phys Med Biol 2009;54:N9-20.
4. Mackie TR, Holmes T, Swerdloff S, Reckwerdt P, Deasy JO, Yang J, *et al.* Tomotherapy: A new concept for the delivery of dynamic conformal radiotherapy. Med Phys 1993;20:1709-19.
5. Jeraj R, Mackie TR, Balog J, Olivera G, Pearson D, Kapatoes J, *et al.* Radiation characteristics of helical tomotherapy. Med Phys 2004;31:396-404.
6. Mackie TR. History of tomotherapy. Phys Med Biol 2006;51:R427-53.
7. Olivera GH, Shepard DM, Reckwerdt PJ, Ruchala K, Zachman J, Fitchard EE, *et al.* Maximum likelihood as a common computational framework in tomotherapy. Phys Med Biol 1998;43:3277-94.
8. Shepard DM, Olivera GH, Reckwerdt PJ, Mackie TR. Iterative approaches to dose optimization in tomotherapy. Phys Med Biol 2000;45:69-90.
9. Niemierko A, Goitein M. The influence of the size of the grid used for dose calculation on the accuracy of dose estimation. Med Phys 1989;16:239-47.
10. Smith CW, Morrey D, Gray K. The influence of grid size on accuracy in radiotherapy dose plotting. Med Phys 1990;17:135-6.
11. Chung H, Jin H, Palta J, Suh TS, Kim S. Dose variations with varying calculation grid size in head and neck IMRT. Phys Med Biol 2006;51:4841-56.
12. Okonogi N, Katoh H, Kawamura H, Tamaki T, Kaminuma T, Murata K, *et al.* Clinical outcomes of helical tomotherapy for super-elderly patients with localized and locally advanced prostate cancer: Comparison with patients under 80 years of age. J Radiat Res 2015;56:889-96.
13. Langen KM, Papanikolaou N, Balog J, Crilly R, Followill D, Goddu SM, *et al.* QA for helical tomotherapy: Report of the AAPM Task Group 148. Med Phys 2010;37:4817-53.
14. International Commission on Radiation Units and Measurements.

Prescribing, Recording, and Reporting Photon-Beam Intensity Modulated Radiotherapy (IMRT). ICRU Report 83. Oxford: Oxford University Press; 2010.
15. Niemierko A. Reporting and analyzing dose distributions: A concept of equivalent uniform dose. Med Phys 1997;24:103-10.
16. Niroomand-Rad A, Blackwell CR, Coursey BM, Gall KP, Galvin JM, McLaughlin WL, *et al*. Radiochromic film dosimetry: Recommendations of AAPM Radiation Therapy Committee Task Group 55. American Association of Physicists in Medicine. Med Phys 1998;25:2093-115.
17. Fuss M, Sturtewagen E, De Wagter C, Georg D. Dosimetric characterization of GafChromic EBT film and its implication on film dosimetry quality assurance. Phys Med Biol 2007;52:4211-25.
18. Low DA, Harms WB, Mutic S, Purdy JA. A technique for the quantitative evaluation of dose distributions. Med Phys 1998;25:656-61.
19. Tomo HD. TomoTherapy Treatment System Tomo Planning, Guide (107272 A). Ver. 1.2.x (white paper) Accuray Incorporated; 2012.